EVS32 **Symposium**
Lyon, France, May 19-22, 2019

Methodology for Modeling a Plugin Hybrid Electric Vehicle Based on Data Logging

Tobias Burgert, Andreas Dollinger, Torben Fischer,

Fraunhofer Institute for Chemical Technology, Pfinztal, Germany

{tobias.burgert,andreas.dollinger,torben.fischer}@ict.fraunhofer.de

Executive Summary

This paper describes the development of a methodology for precise modeling of a plug-in hybrid electric vehicle without having access to any OEC-specific knowledge. The only requirement to apply the methodology is to have the vehicle at hand. As a starting point, an object-oriented physical vehicle model, based on approaches described in the literature, is implemented in the modeling language Modelica. This vehicle model consists of separate sub-models for the vehicle components interfacing each other. Secondly, driving data is recorded using a diagnostic software that accesses the vehicle's sensors via the data link connector (DLC). There is no need to install additional external sensors. The recorded data is used to parameterize all sub-models. As a final step, the sub-models are merged together into an overall vehicle model. The validation of this model is carried out with measurement data from a certified dynamometer. It is shown that this approach leads to an accurate model with a maximal discrepancy of well below 5 % in relevant vehicle parameters. The validated model can then be used for various applications, for example the evaluation of thermal management concepts for hybrid electric vehicles.

1 Introduction

The goal of this study is to develop a methodology to model the longitudinal dynamics of a plug-in hybrid electric vehicle based on data logging. In previous work, components were modeled using maps [1] or physical models [2,3], but not validated on the basis of real measurement data. Alternatively, in other publications [4,5], additional sensors for validation were installed at great expense. This publication shows that the vehicle sensors can be used to obtain the parameters for the modelling as well as to validate the generated model.

The developed approach only requires the vehicle at hand. The methodology comprises the model building described in Sec. 2 based on various approaches detailed in the literature, the acquisition of driving data (Sec. 3) used for the parameterization of the model, and validation (Sec. 4) using measurement data from a certified roller dynamometer. The last section shows an example application of the validated model.

1.1 Vehicle

The AUDI A3 e-tron has been chosen as a reference vehicle. It is a parallel hybrid electric vehicle which is able to draw power from the electric motor (EV mode) or from the electric motor (EM) and the internal combustion engine (ICE) at the same time (hold mode) or to recharge the battery by load point shifting using the ICE (charge mode). The ICE is a direct-injection 1.4-liter four-cylinder gasoline engine with a peak power

of 110kW. The electric motor is a permanently-excited synchronous machine with a peak power of 75 kW. The transmission features an automated 6-speed-dual clutch gearbox. The traction battery consists of prismatic NMC (nickel manganese cobalt oxide) lithium ion cells [6]. It is a series connection of 96 cells, each with a capacity of 25 Ah. This results in a total energy of 8.8 kWh (gross). The electric range is certified to 50 km in the New European Driving Cycle (NEDC).

Table 1: Relevant vehicle parameters.

Parameter	Value
Battery capacity	8.8 kWh
Battery configuration	96s
Electric motor power	75 kW
ICE power	110 kW
Electric range	40 km
Mass m	1850 kg
Drag coefficient c_w	0,32
Frontal Area A	2,13 m^2

2 Vehicle Model

The vehicle model was implemented in the modeling language Modelica, which allows the creation of physical multi-domain models in an object-oriented manner. Each vehicle component is modeled in a sub-model with generic electric, thermal, mechanical and informational interfaces. The sub-models can be assembled together according to the topology of the vehicle being tested. The relevant sub-models are described in the following.

2.1 Battery

The loss mechanisms of Li-ion cells are divided into ohmic losses, transition resistances, electronic and ionic transport in the electrodes, charge transfer losses and diffusion losses [7]. According to the state of the art, a series connection of voltage source, resistor and two RC elements is used to model a battery cell. Extensive tests (e.g. impedance spectroscopy) are necessary to obtain data to parameterize the RC elements, especially if low temperatures are also considered. Consequently, no RC elements are used.

The battery model consists of an equivalent circuit with open circuit voltage (OCV) and internal resistance (R_i). The OCV curve is a function of the state of charge (SOC) and is represented by the following function [8]:

$$V_{OCV} = a + b \cdot (-\ln SOC)^m + c \cdot SOC + d \cdot e^{n(SOC-1)}, \qquad 0 \leq \mathrm{SOC} \leq 1, \mathrm{m} > 0$$

R_i is a function of current (I), SOC and cell temperature (T_{Cell}) and is fitted to a three-dimensional function. The power loss is calculated as follows.

$$P_{loss}^{Cell} = R_i(I, SOC, T_{\mathrm{Cell}}) \cdot I^2$$

Voltage, temperature and current limits are taken into account by the model to prevent damage to the battery (cf. lithium plating). A limitation of the maximum discharging current leads to a reduced acceleration and maximum velocity of the vehicle. A limitation of the maximum charging current decreases the electric range due to a lower maximum regenerative power.

2.2 Power Electronics

IGBTs and antiparallel diodes are used as power semiconductors for electrical traction systems. Losses are mainly divided into switching (sw) and pass-through (pt) losses. The total inverter losses are the result of the individual losses multiplied by the number of semiconductors [9]. Parameters are taken from manufacturer data sheets of comparable performance classes.

$$P_{loss}^{PE} = 6\,(P_{loss,sw}^{IGBT} + P_{loss,sw}^{Diode} + P_{loss,pt}^{IGBT} + P_{loss,pt}^{Diode})$$

Necessary parameters are: Switching frequency, forward voltage of the IGBT and diode, on-resistance of the IGBT and diode, turn-on and turn-off energy losses of the IGBTs, reverse recovery energy of the diode, rated current and rated voltage.

2.3 Electric Motor

The EM is a permanently-excited synchronous machine [10]. The losses of such an EM can be divided into copper losses (cu), iron losses (fe) (hysteresis, eddy current and excess) and friction losses (bearing (brg) and windage (wdge)). Mahmoudi et al. [11] have developed a methodology to approximate loss maps for different types of EMs. It is assumed that the power loss during optimal operation can be expressed as a polynomial function of torque and speed:

$$P_{loss}^{EM}(T,\omega) \approx \sum_{m,n} k_{mn} T^m \omega^n$$

The loss terms have been simplified to the following form for the constant torque (ct) region, see table 2. A quadratic dependence on the torque was additionally used in the constant power region.

Table 2: Classification (k_{mn}) of losses as a function of torque and speed in constant torque and constant power region.

	Constant torque				Constant power			
1	-	fe/brg	-	wdge	-	brg	fe	wdge
T	-	-	-	-	-	-	-	-
T^2	cu	-	-	-	cu	-	cu/fe	-
	1	ω	ω^2	ω^3	1	ω	ω^2	ω^3

The start of the field weakening range is derived from measurement data. The coefficients k_{mn} are determined by solving the following minimization problem separately for the constant torque and constant power range.

$$\min_k \sum_{m,n} ||P_{loss}(T,\omega) - P_{loss}^{meas}(T,\omega)||_2^2$$

2.4 Internal Combustion Engine

The fuel consumption $\dot{m}_{fc}$ is approximated by a polynomial approach as a function of the normalized effective torque T_{norm} and the engine speed n_{norm}.

$$\dot{m}_{fc}(T_{norm}, n_{norm}) \approx \sum_{m,n} j_{mn} {T_{norm}}^m {n_{norm}}^n$$

The coefficients j_{mn} are determined by a minimization problem of least-squares type according to Sec 2.3.

2.5 Chassis Model

Depending on the application case, two different methods to determine the driving resistance are introduced.

On the one hand, the driving resistance F_{roller} comprises the rolling resistance and the drag of the vehicle and is fitted to a polynome of second degree as a function of the velocity.

$$F_{roller} = F_0 + F_1 v + F_2 v^2$$

The coefficients F_0, F_1 and F_2 are determined by solving a minimization problem and may be used directly as target values to adjust the roller dynamometer.

Virtual investigations require a mass-independent determination of the driving resistances. For this purpose a model based on physical equations was used:

$$F_r = F_{air} + F_{rr} = \frac{\rho}{2} c_W \cdot A \cdot v^2 + m \cdot g \cdot c_r(v)$$

The rolling resistance coefficient c_r is approximated by a parabolic function considering its dependence on vehicle speed [18].

$$c_r(v) = \ c_{r0} + \ c_{r1} \cdot v + \ c_{r2} \cdot v^2$$

Using the acceleration force, this leads to:

$$F_a = \ m \ \cdot a = F_r \ = \ F_{air} + F_{rr} = \frac{\rho}{2} c_W \cdot A \cdot v^2 + m \cdot g \cdot c_r(v)$$

The road and wheel specific parameters c_{r0} , c_{r1} and c_{r2} are also determined by using measurement data from a coast down test.

2.6 Driving Cycle

The new emission standard Euro 6d-Temp defines road tests as a mandatory part of the homologation procedure, in addition to tests on the roller dynamometer. This regulation specifies the requirements for the real driving emissions (RDE) test procedure [12]. Within this study an RDE-conform route profile with a total distance of 102 km was defined (30.5 km urban, 28.7 km rural , 42.7 km motorway). It serves as a basis for the upcoming validation.

2.7 Parameter optimization

The parameters of the described powertrain component models are found by using measurement data. For this purpose, an objective function is implemented which consists of the weighted sum of the residual between measurement and model prediction (least squares method).

Thus, the optimization of the parameters is carried out by minimizing the defined objective function. To perform this task, a framework is needed which couples an optimizer with the integration of the simulation model. We chose Python and its modules PyFMI [13] and SciPy [14] due to their convenience and open-source character.

The Modelica model is exported as a Functional Mockup Unit [15] which represents the model in a generic Dynamic Link Library (DLL) with standardized interface functions. This DLL is interfaced by PyFMI, allowing the sequential simulation of the model with different parameter sets. The results are evaluated in the optimizing algorithm, leading to a new parameter set for the simulation. We opted for a Nelder-Mead algorithm [17] as it does not rely on derivative information. It is part of the module SciPy, in which numerous algorithms are available.

3 Measurement Data

The models described in Sec. 2 are parameterized by measurement data acquired using the diagnostic software VCDS [16], allowing the output of the vehicle's sensors to be recorded. The data acquisition is restricted to log only one electric control unit (ECU) at a time. The software is also limited to log a maximum of 12 parameters. The recorded driving data is filtered and classified in preparation for the map fit. Measurement data with a high rate of change is neglected.

3.1 Driving Data

Initially, specific driving manoeuvres were defined to parameterize each sub-model separately. These manoeuvres were carried out in a total of 3.000 km driving data. The acquired data were used to determine the k_{mn} coefficients of the EM model (Sec. 2.3), the j_{mn} coefficients of the ICE model (Sec. 2.4), the fitting coefficients of the battery model for the R_i and OCV functions (Sec. 2.2) and the dynamic wheel radius (Sec. 2.5).

The power loss of the battery is calculated based on data fulfilling stationary conditions. Data without current flow is used to determine the parameters of the OCV curve (Sec. 2.1). On this basis, the power loss is determined (see figure 1), the result is an R^2 of 0.989. The total R^2 of the battery loss fit from -10 °C to +30 °C in 2 degree increments is 0.978.

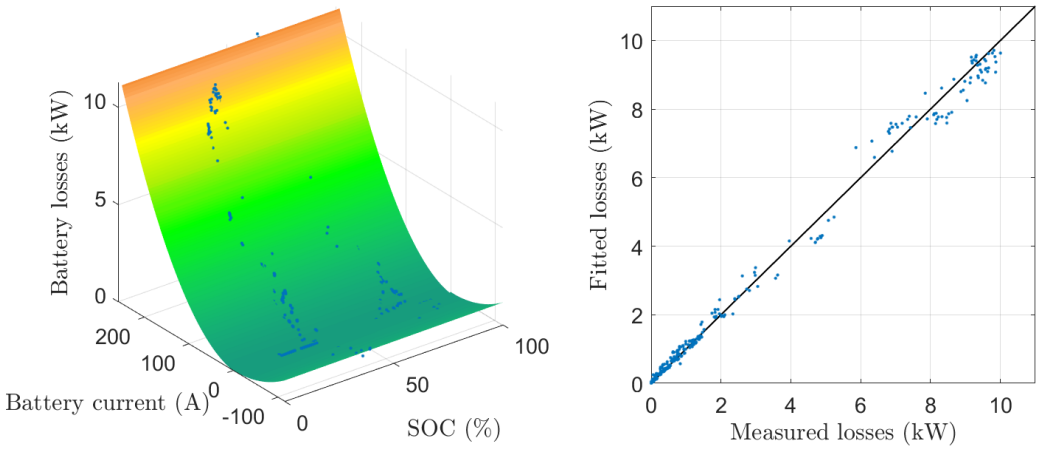

Figure 1: Parameterization of the battery model at 10°C with an R^2 of 0.9956.

The map of the electrical machine is divided into four areas. The constant torque and constant power regions are fitted separately in motor and generator operation. As a transition to the next region, the previously calculated region borders are used as boundary conditions. R^2 is 0.948 for the intire operation range.

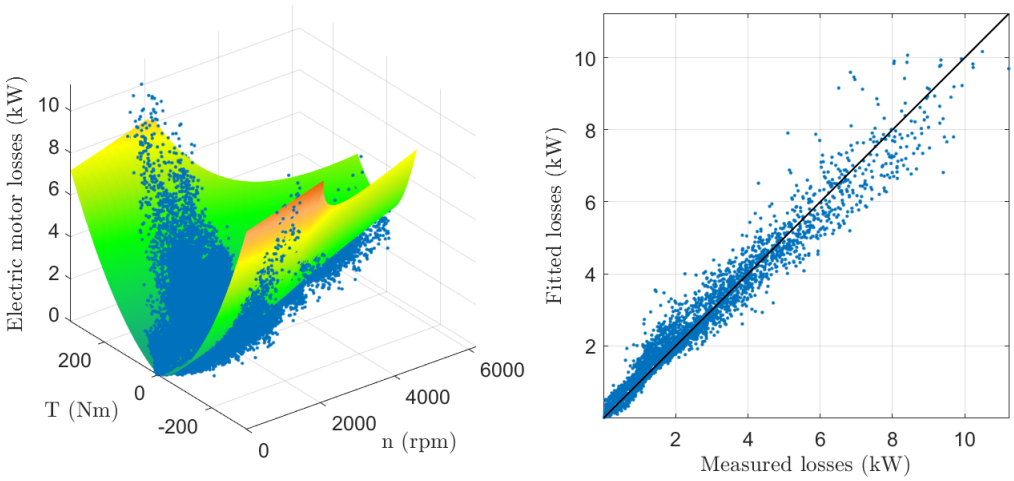

Figure 2: Parameterization of the electric motor model with an R^2 of 0.948.

The fit of the internal combustion engine shows an R^2 of 0.9693. Non-stationary data is neglected in determining the coefficients. The deviation of the measured data relies on rapid load changes and measurement errors of the internal vehicle sensors as well as an inaccuracy of the calculated engine torque.

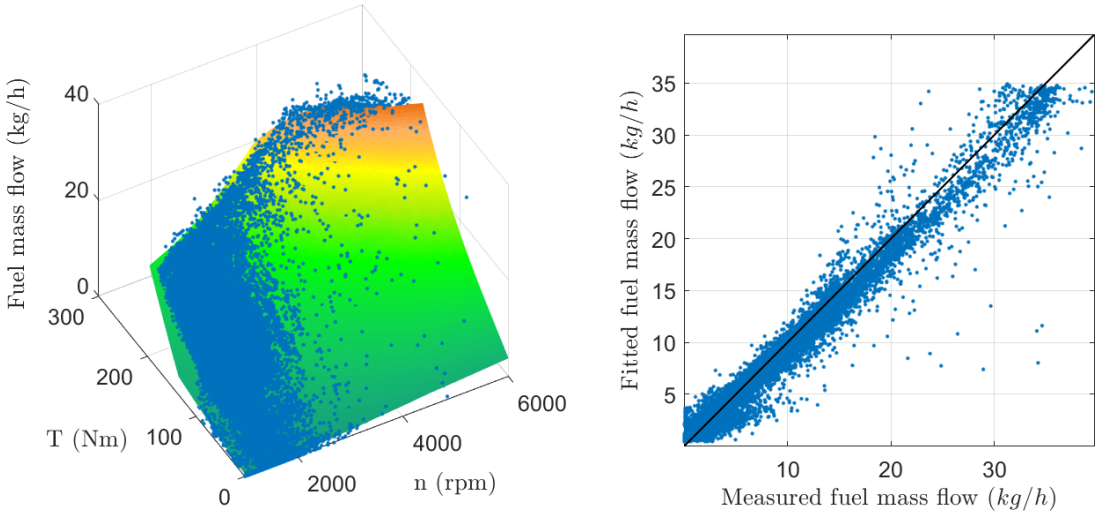

Figure 3: Parameterization of the internal combustion engine model with an R^2 of 0.9693.

The gear shifting points of the automatic transmission depend on the operating mode, accelerator pedal position and input speed. We identified the engaged gear and the input speed as the dominant factors in the driving data and extracted upper and lower shifting points for each gear (see table 3).

Table 3: Shifting points of the gearbox.

Speed	Shifting up	Shifting down
1	2,000 rpm	-
2	2,400 rpm	1,100 rpm
3	2,400 rpm	1,400 rpm
4	2,300 rpm	2,000 rpm
5	4,200 rpm	1,600 rpm
6	-	1,500 rpm

The coefficients F_0, F_1 and F_2 of the driving resistance (Sec. 2.5) were determined by coast down tests (see table 4).

Table 4: Driving resistance coefficients.

Coefficient	Value
F_0	200 N
F_1	0.2 N/(km/h)
F_2	0.037 N/(km/h)^2

In these tests the vehicle is accelerated to a defined velocity on a flat road before being coasted down to a full vehicle stop. These tests are performed multiple times and in both driving directions to account for different external influences such as wind speed, wind direction, rolling resistance and slope. Using these results and the vehicle parameters given in table 1, the road and wheel specific parameters may be calculated (see table 5).

Table 5: The rolling resistance coefficients.

Coefficient	Value
c_{r0}	1.00E-02
c_{r1}	1.00E-05 1/(km/h)
c_{r2}	1.64E-07 1/(km/h)^2

3.2 Climate Chamber

We also cooled down the vehicle and its battery in a climate chamber to explore the current limitations of the battery. The battery charge and discharge current is limited depending on cell temperature and state of charge, to prevent damage to the battery (cf. lithium plating). The maximum discharging current is directly linked to the maximum power of the motor and thus has a significant influence on the acceleration and maximum velocity of the vehicle. The maximum charging current is directly linked to the maximum regenerative power when braking, and affects the electric range.

The temperature and the SOC were varied, resulting in a three-dimensional map. Figure 4 shows the maximum charging and discharging currents of the battery which are limited by the vehicle's control unit.

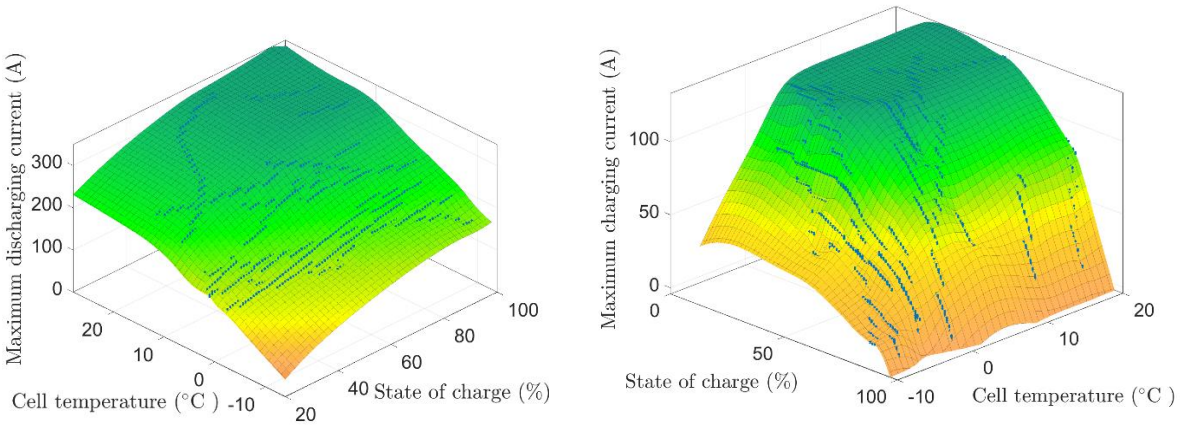

Figure 4: Maximum battery charging and discharging currents depending on state of charge and temperature.

The limitation of the charging current begins above a state of charge of 55 % and below a cell temperature of 0 °C. The charging current is further decreased with increasing state of charge and decreasing temperature, whereby a state of charge of 90 % and a temperature of -15 °C mark the disabling of the regenerative braking feature.

4 Validation

The parameterized sub-models were merged together in an overall vehicle model, which is validated by measurement data logged on a certified roller dynamometer. The velocity profile was recorded on the previously defined RDE driving route. Thermal conditioning of the vehicle is deactivated and the ambient temperature is conditioned to 23 °C.

Table 5: Validation of the model against measurement data

Parameter	Unit	Simulation	Measurement	Deviation
Total distance	km	101.84	102.04	-0.17 %
Fuel consumption	l	3.87	3.78	+2.4 %
Energy consumption	kWh	6.01	5.91	+3.06 %
CO_2 mass	kg	9.01	8.74	+1.66 %
Electric range	km	33.2	33.31	-0.32 %

Table 5 shows the resulting deviation between the simulation model and measurement data in regard to relevant parameters. We observe a very small discrepancy in the total travelled distance and the electric range. This demonstrates that the electric powertrain is modeled very precisely. The slightly higher deviation in terms of fuel consumption and CO_2 emissions is largely attributable to the unknown load point shifting strategy in the hold mode of the vehicle. Nevertheless, these deviations are considered to be in an acceptable range.

5 Virtual Investigation

The effect of different battery cell temperatures is investigated in the following section. Figure 5 shows the same part of the RDE-cycle for battery temperatures of -10 °C and +10 °C. On the one hand, the same electric power demand leads to a higher required battery current, since the internal resistance increases at low battery temperatures. On the other hand, the maximum battery charge current (black dotted line) decreases at low temperatures, leading to a reduction of the energy recovered.

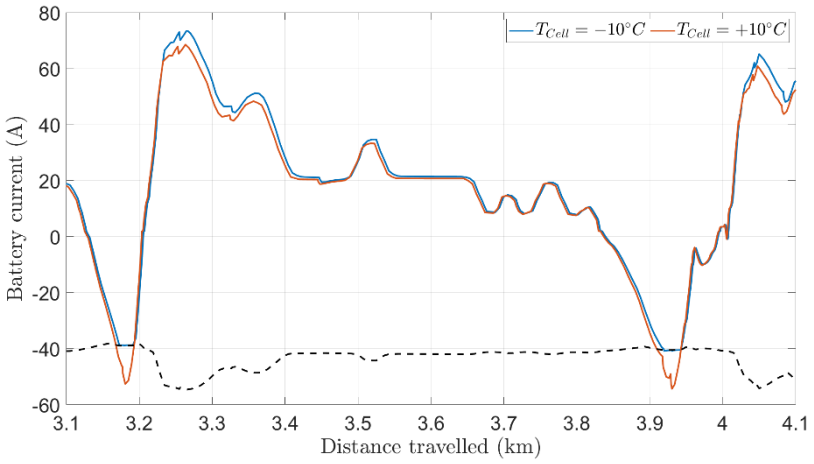

Figure 5: Comparison of a the battery current in the RDE cycle at -10 °C and 10 °C battery temperature. At low temperatures, more current is needed to achieve the same power, and maximum recuperative power is limited (dotted line).

Next, the cell temperature is varied from +10 °C to -10 °C and is assumed to be constant. Figure 6 shows the results.

Due to the rising internal resistance with decreasing cell temperature, the electric range is reduced, which leads to a higher fuel consumption and CO_2 emissions in the defined driving cycle. Furthermore, regenerative braking is limited at low cell temperatures, as seen in Sec. 3.1.

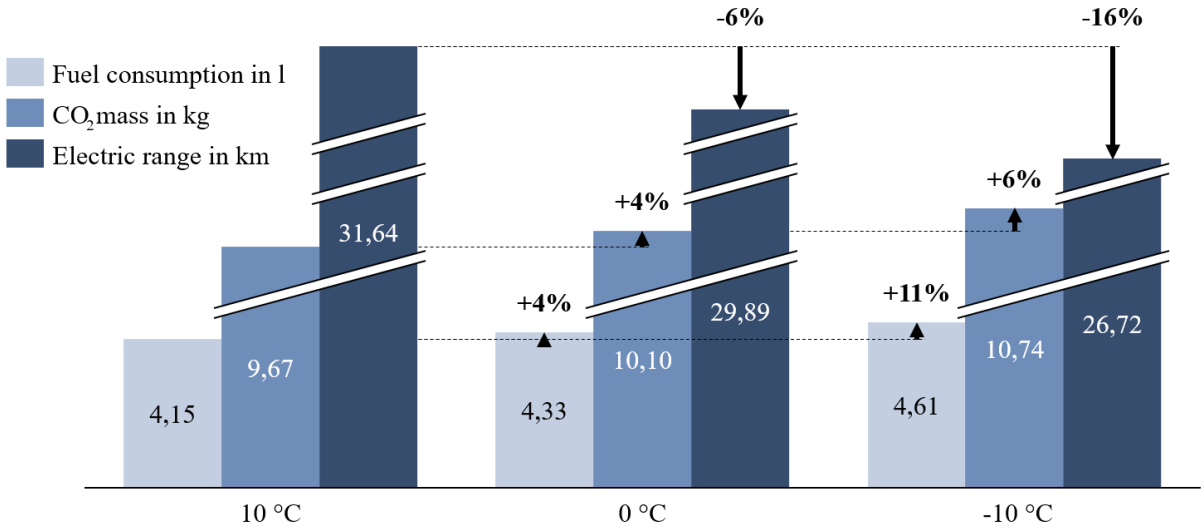

Figure 6: Results of virtual investigation depending on ambient temperature.

6 Conclusion

This paper describes a methodology to model the longitudinal dynamics of a plug-in hybrid electric vehicle based on logging sensor data from the vehicle. This data is used to obtain the parameters for modelling the hybrid drive train. The method is applied with a vehicle diagnostic tool using an Audi A3 e-tron. In addition to real driving data, measurements in a climatic chamber were used to further optimize the model.

Relevant factors influencing the recuperable performance, such as the increasing power loss of the battery and the maximum charging current at low temperatures, were presented. The overall vehicle model consisting of the interfacing sub-models was finally validated, and shows a deviation of less than 5 % compared to measurement data of a roller dynamometer. The influence of battery temperature on fuel consumption, CO_2 emissions and electrical range was shown in a virtual study.

The developed model serves as a reference for the status quo and can be used to evaluate vehicle modifications in terms of fuel consumption, electric range and CO_2 emissions.

Acknowledgements

This publication was written in the framework of the Profilregion Mobilitätssysteme Karlsruhe, which is funded by the Ministry of Science, Research and the Arts and the Ministry of Economic Affairs, Labour and Housing in Baden-Württemberg and as a national High Performance Center by the Fraunhofer-Gesellschaft.

References

[1] A. Boukehili et al., *Parallel HEV Hybrid Controller Modeling for Power Management,* 25th International Electric Vehicle Symposium (EVS25), Shenzhen, China, 2010

[2] S. Evangelou, *Dynamic modeling platform for series hybrid electric vehicles*, Department of Electrical and Electronic Engineering, Imperial College London, UK, 2016

[3] D. Gao et al., *Modeling and Simulation of Electric and Hybrid Vehicles,* Proceedings of the IEEE 5(4):729 - 745 · May 2007

[4] Pasquier et al., *Validating Simulation Tools for Vehicle System Studies Using Advanced Control and Testing Procedure*, 18th International Electric Vehicle Symposium (EVS18), Berlin, 2001

[5] Ahmed, M. and Naiju, C., *Modeling and Simulation for Hybrid Electric Vehicle with Parallel Hybrid Braking System for HEV*, SAE Technical Paper 2018-28-0097, 2018

[6] F.L.Mapelli and D. Tarsitano, *Modeling of Full Electric and Hybrid Electric Vehicles*, Intech Open Access Publisher, DOI: 10.5772/5357, 2012

[7] J.P. Schmidt, *Verfahren zur Charakterisierung und Modellierung von Lithium-Ionen-Zellen*, Karlsruhe Institute of Technology, 2013

[8] Zhang et al., *A Generalized SOC-OCV Model for Lithium-Ion Batteries and the SOC Estimation for LNMCO Battery,* MDPI, Basel, Switzerland 2016

[9] D. Pohlenz, *Wirkungsgradoptimale Regelung eines elektrischen Fahrantriebes mit variabler Zwischenkreis-spannung,* Dissertation, Universität Paderborn, 2012

[10] H. Jelden et al., *Der Plug-In Hybrid des modularen Querbaukastens von Volkswagen*, MTZ – Motortechnische Zeitschrift, Number 04, 2014

[11] Mahmoudi et al., *Loss Function Modeling of Efficiency Maps of Electrical Machines*, IEEE Transactions on Industry Applications

[12] Commission Regulation (EU) 2016/427, Visited: 24.10.2018, URL: https://eur-lex.europa.eu/legal-content/EN/TXT/ HTML/?uri=CELEX:32016R0427&from=DE

[13] Andersson, C., Åkesson, J., & Führer, C. (2016). *PyFMI: A Python Package for Simulation of Coupled DynamicModels with the Functional Mock-up Interface.* (Technical Report in Mathematical Sciences; Vol. 2016, No. 2).Centre for Mathematical Sciences, Lund University.

[14] Jones E, Oliphant E, Peterson P, et al. *SciPy: Open Source Scientific Tools for Python*, 2001-, http://www.scipy.org/ [Online; accessed 2019-03-15].

[15] T. Blochwitz, et al. *Functional Mockup Interface 2.0: The Standard for Tool Independent Exchange of Simulation Models*, Proceedings of the 9th International Modelica Conference, September 3-5, 2012, Munich, Germany

[16] VCDS Diagnostic Software, Visited: 24.10.2018, URL: http://www.ross-tech.com

[17] J.A. Nelder et al., *A Simplex Method for Function Minimization*, The Computer Journal*, Volume 7, Issue 4, 1 January 1965, Pages 308–313*

[18] J. Páscoa, et al. (2012). *An innovative experimental on-road testing method and its demonstration on a prototype vehicle*. Journal of Mechanical Science and Technology. 26. 10.1007/s12206-012-0413-8.

Authors

Tobias Burgert obtained a degree in Mechanical Engineering within the scope of a double diploma program at the Karlsruhe Institute of Technology (KIT) and the Institut des Sciences Appliquées de Lyon (INSA). He is a research associate at the Fraunhofer Institute for Chemical Technology (ICT) since 2013 and focuses on vehicle models and data logging.

Andreas Dollinger received his B.Sc. and M.Sc. in Electrical Engineering from the Karlsruhe Institute of Technology (KIT) in 2012 and 2014. He currently works on motor drive applications for electric and hybrid electric vehicles at the Fraunhofer Institute for Chemical Technology (ICT).

Torben Fischer obtained a degree in Mechanical Engineering within the scope of a double diploma program at the Karlsruhe Institute of Technology (KIT) and the Institut des Sciences Appliquées de Lyon (INSA). He is a PhD student at the Fraunhofer Institute for Chemical Technology (ICT) dealing with thermodynamic simulations in the context of automotive systems. This comprises thermal management systems with heat pumps and A/C cycles, as well as heat recovery systems.